Diversity of Uranium Reduction Processes in Oak Ridge Source Zone Sediment

Jennifer L. Nyman[1], Terence L. Marsh[2], Matt Ginder-Vogel[3], Scott Fendorf[3], and Craig Criddle[1]

[1]Department of Civil and Environmental Engineering, Stanford University, Stanford, CA; [2]Center for Microbial Ecology, Michigan State University, East Lansing, Michigan; [3]Department of Geological and Environmental Sciences, Stanford University, Stanford, CA

Motivation: Field-Scale Bioremediation

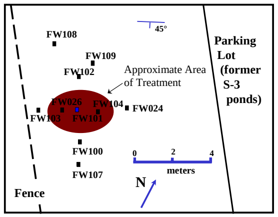

Figure 1. Location of the Near-Source Zone Biostimulation Experiment and Associated Wells.

Subsurface Contamination Near the Source Zone:

› low pH (~3.6)

› high uranium, sulfate, nitrate

› co-contaminants, including technetium, VOCs, and chromium

Field-Scale Treatment Strategy:

› displacement of nitrate and acidity

› above-ground denitrification in a fluidized bed reactor (FBR)

› ethanol addition to stimulate *in-situ* denitrification and microbial U(VI) reduction

Experimental Approach

The scale-up of microbial uranium reduction from the bench scale to the the field scale presents several challenges, so microcosms were established with sediment from near the source zone to simulate the conditions of the field experiment.

Microcosm Setup:

› washed sediment from well 103 (40 ft)

› denitrified synthetic groundwater

› ethanol (22 mM)

› the effluent of a pilot denitrifying FBR

› one-half autoclaved as controls

Sacrificed Sediment:

› sets of microcosms sacrificed on days 1, 14, 27, 63, and 93

› community structure by T-RFLP using the 16S rRNA gene

› X-ray absorption near-edge structure (XANES) spectroscopy for oxidation state of metals

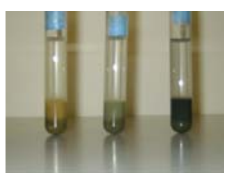

Figure 2. Color Change in Microcosms Over Time. The color of sediment and solution in microcosms turned from brown to gray to black, indicating the establishment of reducing conditions.

Conclusions

› Under sediment and groundwater conditions representative of the source zone during treatment, the amendment of ethanol stimulated microbial uranium reduction. This transformation was apparently mediated by bacterial activity, as uranium was not reduced in sterilized microcosms.

› Various soluble uranium concentration patterns highlight the significance of small-scale sediment and/or inoculum heterogeneity. Field-scale experimental results will likely be a composite of variable reaction rates on this dimension.

› A rebound in uranium concentration suggests biological reduction rates had decreased until they were less than uranium desorption rates from the solid phase. As ethanol, acetate, and sulfate were depleted in microcosms with rebounding uranium concentration, the rate of microbial uranium reduction may have been limited by a lack of electron donor or acceptor.

› Uranium was reduced concurrently with sulfate, perhaps due to greater bioavailability of soluble sulfate over ferric iron or due to greater initial numbers of sulfate-reducing bacteria in the inoculum.

› T-RFLP indicated a shift in community structure as uranium was reduced, although the *Hha*I and *Msp*I profiles were each dominated by one or two fragment lengths.

Uranium Reduction Patterns

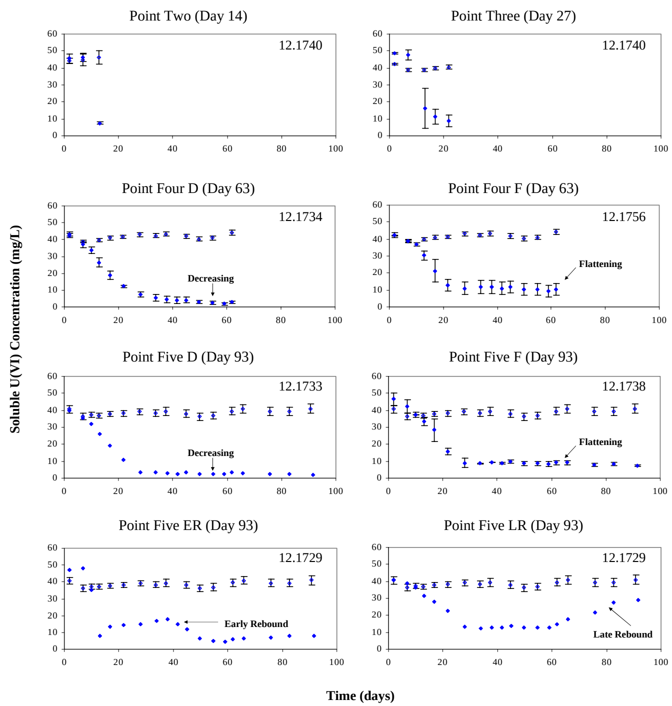

Figure 3 (above). Soluble U(VI) Concentration. U(VI) concentration is shown for control (open symbols) and viable (closed symbols) microcosms over time. Chart titles indicate the day on which the microcosms were sacrificed and the sample name of the sediment. Though U(VI) concentration decreased steadily in most microcosms, in others it leveled off or rebounded.

The U binding energy, as determined by XANES, is shown for each viable sediment sample at the top right of the graph. U(VI) has a slightly higher L_{III}-shell (2p orbital) binding energy than U(IV) (17.176 vs. 17.172 keV), so a low relative binding energy indicates the reduction of solids-associated uranium.

XANES

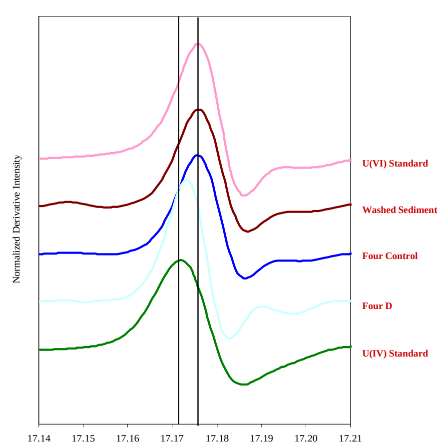

Figure 4 (left). Representative XANES Spectra. Spectra for U(VI) and U(IV) standards, washed sediment, and representative samples are shown. XANES analysis indicated little solids-associated iron was reduced in viable microcosms while all chromium was reduced.

Electron Donor and Acceptor Concentrations

Sample	Nitrate (mM) Control	Nitrate (mM) Viable	Sulfate (mM) Control	Sulfate (mM) Viable	Acetate (mM) Control	Acetate (mM) Viable	Ethanol (mM) Control	Ethanol (mM) Viable
Point One	1.1 (0.04)	0.1 (0.1)	3.3 (0.3)	3.0 (0.4)	bd	bd	21.2 (2.6)	21.4 (3.7)
Point Two	1.0 (0.2)	0.04 (0.02)	3.2 (0.7)	0.1 (0.05)	bd	11.4 (1.0)	23.0 (3.9)	1.5 (0.8)
Point Three	1.6 (0.4)	bd	3.4 (1.3)	0.1 (0.2)	bd	13.5 (2.4)	21.7 (5.0)	bd
Point Four: D	1.2 (0.1)	bd	4.1 (0.6)	2.3 (0.5)	bd	14.0 (2.1)	21.3 (1.5)	bd
F		bd		1.7 (0.9)		13.2 (2.5)		bd
Point Five: D	1.2 (0.2)	bd	4.0 (0.8)	2.7	bd	18.4	17.7 (1.9)	bd
F		bd		1.4		28.3		bd
ER		bd		bd		bd		bd
LR		bd		bd		bd		bd

Table 1. Electron Donor and Acceptor Concentrations. In viable microcosms, ethanol concentration decreased as acetate accumulated, nitrate was depleted within two weeks, and sulfate concentration decreased concurrently with uranium reduction. Standard deviations are shown in parentheses. bd = below detection limit.

Community Analysis

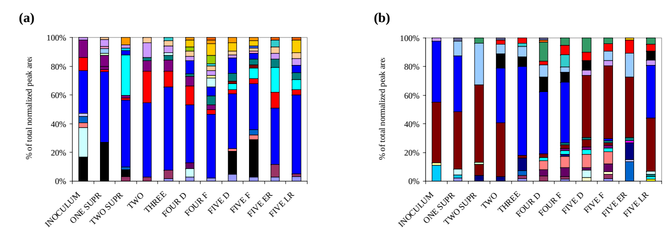

Figure 5. Composition of T-RFLP profiles. Histograms show the contribution of terminal restriction fragments to the percentage of total normalized peak height for 16S rDNA digested with the tetrameric enzymes *Hha*I (a) and *Msp*I (b). One to two restriction fragment lengths dominate most profiles, but significant variation exists in the relative proportion of other lengths.

Figure 6. Cluster Diagrams of T-RFLP profiles. Normalized peak heights for fragments were transformed by taking their square root, and then profiles were clustered with either unweighted pair group method mean average (UPGMA) (a) or Ward's (b) methods. Diagrams indicate a general shift in community structure occurred as uranium was reduced, and, except for sample Five LR, samples with variable patterns of uranium reduction but from the same time point clustered together.

Acknowledgements

› This work was funded by the National Science Foundation graduate fellowship program and United States Department of Energy (DOE) National and Accelerated Bioremediation Research (NABIR), Biological and Environmental Research (BER) (grant #DE-F603-00ER63046).

› X-ray analysis was performed at the Advanced Photon Source (APS) and the Stanford Synchrotron Radiation Laboratory (SSRL).

› We would like to thank David Watson of the Oak Ridge Field Research Center for providing samples.